

Chapter 5: Spectral Synthesis

5.1: Requirements of Spectral Synthesis

The emergent spectrum from a portion of the photosphere is the specific intensity at $\tau = 0$. Thus, the calculation of an emergent spectrum (**spectral synthesis**) requires the (numerical) solution of the radiative transfer equation (equation (3-11)).

$$\mu \frac{dI_\lambda}{d\tau_\lambda} = I_\lambda - S_\lambda. \quad (5-1)$$

Given suitable boundary conditions for this differential equation, and given the source function $S_\lambda(\tau_\lambda)$, the solution is reasonably straightforward.

For the boundary conditions, we can assume that the radiation incident upon the surface of the sun is negligible, and that at a sufficiently great depth, the photosphere and the radiation field are in thermodynamic equilibrium. The depth required for thermodynamic equilibrium to hold is small compared to the radius of the sun, so the plane-parallel radiative transfer equation is entirely suitable.

The variation of the source function with optical depth is also required. For LTE cases, we can assume that

$$S_\lambda(z) = B_\lambda(z). \quad (5-2)$$

As the Planck radiation function B_λ is a function of temperature and wavelength only, if the variation of temperature with physical height z in the photosphere is known, the source function can be found at all points. The source function at all optical depths is required for the solution of the transfer equation, so the optical depth as a function of height must also be known. This is given by equation (3-10):

$$\tau_\lambda(z) = \int_z^\infty \rho(z') \kappa_\lambda(z') dz'. \quad (5-3)$$

To find the optical depth, the opacity must be known.

To find the opacity, information on the state of the photosphere and data for any relevant atomic transitions are required. Given this data, it is possible to calculate the emergent spectrum from the sun.

Only the LTE plane-parallel case will be considered here. Non-plane-parallel conditions (due to inhomogeneities) can be treated as an ensemble of plane-parallel regions, and are treated in detail in chapter 8. Cases with significant departures from LTE are avoided in this work.

5.2: Basic Procedures For Plane-Parallel Spectral Synthesis

5.2.1: The LTE Approximation

The greatest difficulty in spectral synthesis in the general (ie non-LTE) case will be in determining atomic level populations. The populations will depend on the radiation field; the radiation field will depend on the level populations. If the radiation field at some depth in the photosphere is known, and the level populations at this point are known, this provides the necessary boundary condition for solution of the transfer equation. Since collision rates increase with depth, at some point, a depth must be reached at which the atmosphere is in (approximately) LTE, and at this depth the level populations will be given by the Boltzmann distribution. As the opacity also increases with depth, the radiation field interacts with a smaller and smaller region of the photosphere, until it can also be considered to be in thermal equilibrium with the photosphere. Thus, the radiation field will be given by the Planck function.

Unfortunately, if we just proceed to numerically integrate to determine the radiation field at nearby points, and use this to find the new populations, small errors will tend to accumulate and exponentially grow. Suitable choice of an algorithm capable of giving an accurate answer becomes important. Typically, an iterative technique in which certain level populations are assumed and then adjusted according to the radiation fields that are found to be present. The new populations can then be

used to determine a new radiation field, and so on. Such algorithms and the speed of their convergence form a large part of the literature on spectral synthesis.¹

Obviously, if the level populations could be known, *a priori*, the problem would be much simpler. Thus, the LTE approximation is extremely attractive.

5.2.2: Calculation of Opacities

In the LTE approximation, the level populations and the ionisation balance are simply functions of the local temperature, and therefore the opacity is a function of the temperature as well, and is independent of the radiation field.

In general, to find the opacity, the contributions to the opacity from all sources of absorption must be added:

$$\kappa_{\lambda} = \kappa_1(\lambda) + \kappa_2(\lambda) + \dots \quad (5-4)$$

where κ_1 etc are the contributions from various processes. These processes can be grouped into line and continuum processes, so

$$\kappa_{\lambda} = \kappa_{\lambda c} + \kappa_{\lambda \ell} \quad (5-5)$$

Finding the opacity due to a process involves finding the absorption cross-section for a single absorber, and using the number of eligible absorbers per gram to convert the cross-section to an opacity.

¹See Crivellari, L., Hubeny, I. and Hummer, D.G. (eds) “Stellar Atmospheres: Beyond Classical Models” *NATO ASI (Advanced Science Institute) Series, Series C: Mathematical and Physical Sciences* **341**, Kluwer Academic Publishers, Dordrecht (1991) for a number of examples. While NLTE cases can generally be avoided for the photosphere, the NLTE cases can be of interest themselves. NLTE techniques are also useful for treating radiative transfer in structures such as spicules, prominences and loops. See Heinzel, P. “Multilevel NLTE Radiative Transfer in Isolated Atmospheric Structures: Implementation of the MALI-Technique” *Astronomy and Astrophysics* **299**, pg 563-573 (1995) for a discussion of such problems. NLTE calculations generally involve a technique known as Accelerated Lambda Iteration (ALI).

5.3: The Continuous Opacity

As stated in chapter 3, the main contribution to the continuous opacity is due to bound-free and free-free H^- transitions. Other important contributions are due to bound-free and free-free absorption by atomic hydrogen (due to its high abundance). Contributions due to the H_2^+ molecule and photoionisation of abundant elements such as silicon and magnesium are also considered.

5.3.1: H^- Ion Opacity

The H^- ion can absorb photons through both bound-free and free-free processes, namely



for bound-free transitions and



for free-free transitions.

The determination of the interaction cross-sections for these two processes is difficult, but accurate calculations have been performed.²

The bound-free H^- opacity is given in terms of the absorption cross section by

$$\kappa_{\lambda H^-(bf)} = \frac{N_{H^-}}{\rho} \alpha_{\lambda H^-(bf)} \quad (5-8)$$

where N_{H^-} is the H^- number density.

The H^- ion population can be found in terms of the neutral hydrogen population by using Saha's equation (equation 2-21), giving

$$\frac{N_H N_e}{N_{H^-}} = \left(\frac{2\pi m_e kT}{h^2} \right)^{\frac{3}{2}} \frac{2U_H(T)}{U_{H^-}(T)} e^{-\chi_i/kT}. \quad (5-9)$$

²See Geltman, S. "The Bound-Free Absorption Coefficient of the Hydrogen Negative Ion" *The Astrophysical Journal* **136**, pg 935-945 (1962) for bound-free absorption and Geltman, S. "Continuum States of H^- and the Free-Free Absorption Coefficient" *The Astrophysical Journal* **141**, pg 376-394 (1965) for free-free absorption.

Writing this in terms of the electron pressure given by

$$P_e = N_e kT \quad (5-10)$$

and combining all of the temperature dependent terms into a single function $\phi(T)$, the H^- population is given by

$$N_{H^-} = N_H P_e \phi(T) \quad (5-11)$$

which can be substituted into equation (5-8) to give the bound-free opacity

$$\kappa_{\lambda H^-(bf)} = \frac{N_H}{\rho} P_e \phi(T) \alpha_{\lambda H^-(bf)} \quad (5-12)$$

or, correcting for stimulated emission,

$$\kappa_{\lambda H^-(bf)} = \frac{N_H}{\rho} P_e \phi(T) \alpha_{\lambda H^-(bf)} (1 - e^{-hc/\lambda kT}). \quad (5-13)$$

This can be calculated using the approximation formulae for $\phi(T)$ and $\alpha_{\lambda H^-(b-f)}$ given by Gingerich.³ These give

$$\phi(\theta) = 0.4158 e^{1.726\theta} \theta^{\frac{5}{2}} \quad (5-14)$$

where $\theta = \frac{5040^\circ \text{K}}{T}$ and

$$\alpha_{H^-(b-f)} = 6.80133 \times 10^{-3} + 0.178708 \lambda + 0.164790 \lambda^2 - 2.04842 \times 10^{-2} \lambda^3 + 5.95244 \times 10^{-4} \lambda^4 \quad (5-15)$$

where the wavelength λ is in thousands of Ångströms, giving the absorption coefficient per unit electron pressure in units of $10^{-26} \text{ cm}^4 \text{ dyn}^{-1}$.

The free-free opacity will depend on the population of dissociated H^- ions (which are neutral hydrogen atoms) and on the population of free electrons. Gingerich⁴ gives an approximation formula for the absorption coefficient per unit electron pressure per hydrogen atom, including the correction factor for stimulated emission

³See pg 17, Harvard-Smithsonian Conference on Stellar Atmospheres "Proceedings of the First Conference" *Smithsonian Astrophysical Observatory Special Report 167*, Smithsonian Astrophysical Observatory, Cambridge (1964).

⁴In Harvard-Smithsonian Conference on Stellar Atmospheres "Proceedings of the First Conference" *Smithsonian Astrophysical Observatory Special Report 167*, Smithsonian Astrophysical Observatory, Cambridge (1964).

$$\begin{aligned} \alpha_{\text{H}^-(\text{ff})} = & (5.3666 \times 10^{-3} - 1.1493 \times 10^{-2} \theta + 2.7039 \times 10^{-2} \theta^2) \\ & + (-3.2062 \times 10^{-3} + 1.1924 \times 10^{-2} \theta - 5.9390 \times 10^{-3} \theta^2) \lambda \\ & + (-4.0192 \times 10^{-4} + 7.0355 \times 10^{-3} \theta - 3.4592 \times 10^{-4} \theta^2) \lambda^2 \end{aligned} \quad (5-16)$$

where the result is in units of $10^{-26} \text{ cm}^4 \text{ dyn}^{-1}$.

The total H^- opacity is then given by

$$\kappa_{\lambda\text{H}^-(\text{bf})} = \frac{N_{\text{H}}}{\rho} P_e \left(\phi(T) \alpha_{\lambda\text{H}^-(\text{bf})} (1 - e^{-hc/\lambda kT}) + \alpha_{\lambda\text{H}^-(\text{ff})} \right). \quad (5-17)$$

The variation of the H^- opacity with wavelength and height within the photosphere is shown in figure 5-1 below.

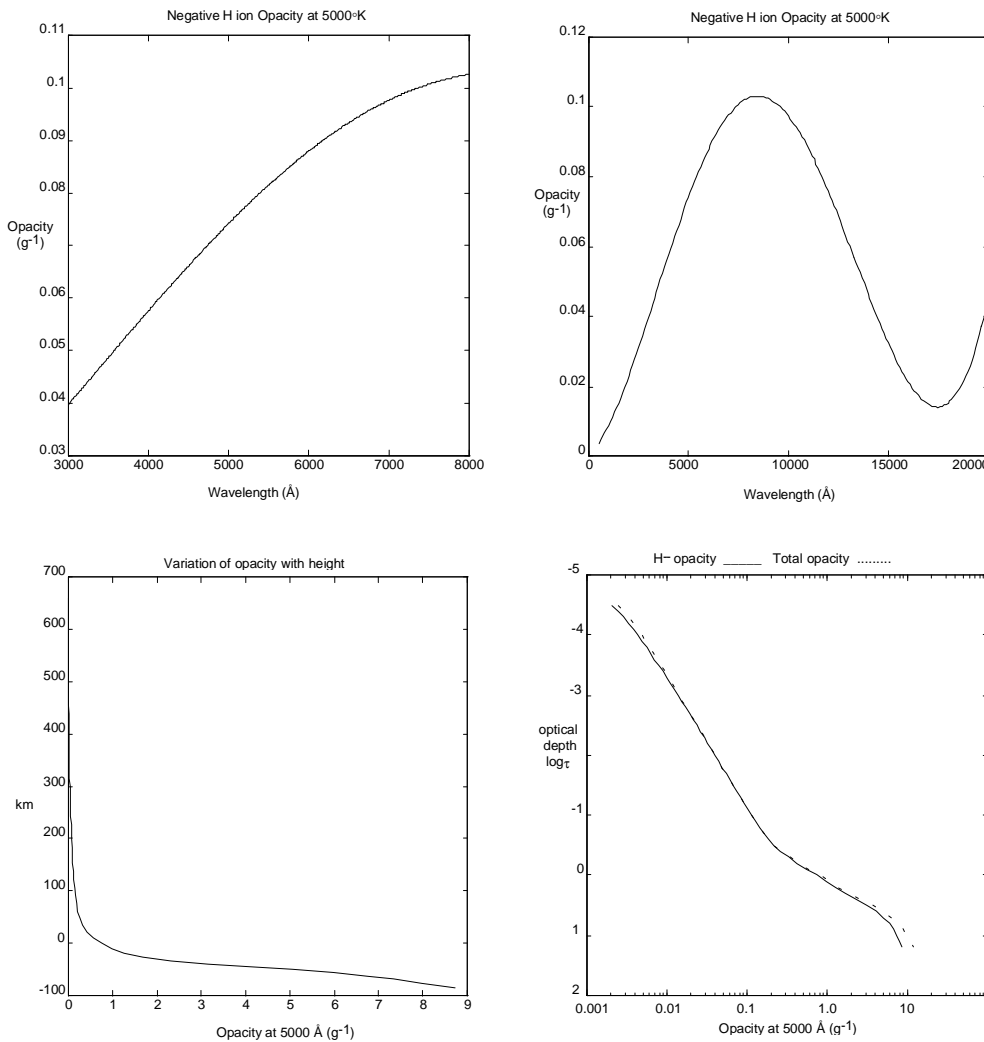


Figure 5-1: The H^- Opacity

From figure 5-1, it can be seen that H^- opacity is very much the dominating contribution to the visible opacity in the photosphere. At 5000 Å, it is only slightly below the total opacity.

5.3.2: Bound-Free Hydrogen Opacity

The quantum number n of a bound hydrogen energy state is given by the Rydberg equation

$$E_n = -\frac{E_R}{n^2} \quad (5-18)$$

where E_R is the Rydberg energy, or Bohr energy, ($E_R = 13.6 \text{ eV} = 109\,677 \text{ cm}^{-1}$ for hydrogen) and E_n is the energy of the state, with the ionisation energy taken to be zero.

In a similar manner, an imaginary quantum number ik can be defined for continuum states where

$$E_k = \frac{1}{2} m_e v^2 = \frac{E_R}{k^2}. \quad (5-19)$$

The wavelength for a photoionisation event is then

$$\frac{hc}{\lambda} = E_R \left(\frac{1}{n^2} + \frac{1}{k^2} \right). \quad (5-20)$$

The problem can then be treated identically to bound-bound transitions in hydrogen (see section A.2.1 in appendix A for the bound-bound oscillator strength for hydrogen). The oscillator strength of the transition can be found by substituting the imaginary quantum number ik into equation (A-10) (the equation for the bound-bound oscillator strength) giving

$$f_{nk} = \frac{32}{3n^2} \frac{e^{-4k \tan^{-1}(n/k)} |\Delta(n, ik)|}{k^3 n^3 \left(\frac{1}{n^2} + \frac{1}{k^2} \right)^{\frac{7}{2}} (1 - e^{-2\pi k})} \quad (5-21)$$

where $\Delta(n, ik)$ is the same function as given in equation (A-15). This oscillator strength can then be written in terms of an appropriate Gaunt factor g_{II} as

$$f_{nk} = \frac{32}{3\pi\sqrt{3}} \frac{1}{n^5 k^3} \left(\frac{1}{n^2} + \frac{1}{k^2} \right)^{-3} g_{II}(n, k) \quad (5-22)$$

where

$$g_{\text{II}} = \pi \sqrt{3} k n e^{-4k \tan^{-1}(n/k)} \frac{|\Delta(n, ik)|}{\sqrt{k^2 + n^2 (1 - e^{-2\pi k})}}. \quad (5-23)$$

The total absorption cross-section for a transition in terms of the f-value is then given by equation (3-41)

$$\sigma_{nk} = \frac{\pi e^2}{m_e c} f_{nk}. \quad (5-24)$$

In a small wavelength interval $d\lambda$, there must be dk continuum states. The total absorption cross-section for an atom in state n at a wavelength λ must be

$$\alpha_{n\lambda} = \sigma_{nk} \frac{\lambda^2}{c} \frac{dk}{d\lambda} \quad (5-25)$$

if the wavelength interval $d\lambda$ is small enough so that σ_{nk} can be considered as constant over the interval.⁵ The density of continuum states can be found from equation (5-20)

$$\frac{dk}{d\lambda} = \frac{hck^3}{2E_R \lambda^2} \quad (5-26)$$

giving an absorption cross-section of

$$\begin{aligned} \alpha_{n\lambda} &= \frac{\pi e^2}{m_e c} \frac{32}{3\pi \sqrt{3}} \frac{1}{n^5 k^3} \left(\frac{1}{n^2} + \frac{1}{k^2} \right)^{-3} g_{\text{II}}(n, k) \frac{\lambda^2}{c} \frac{hck^3}{2E_R \lambda^2} \\ &= \frac{\pi e^2}{m_e c} \frac{32}{3\pi \sqrt{3}} \frac{1}{n^5 k^3} \left(\frac{hc}{E_R \lambda} \right)^{-3} g_{\text{II}}(n, k) \frac{hk^3}{2E_R} \\ &= \frac{16}{3\sqrt{3}} \frac{e^2 E_R}{m_e h^2 c^2} \frac{g_{\text{II}}(n, k)}{n^5} \lambda^3 \\ &= 1.0435 \times 10^{-2} \frac{g_{\text{II}}(n, k)}{n^5} \lambda^3. \end{aligned} \quad (5-27)$$

The longest wavelength that can be absorbed in a bound-free process is that with the energy needed to reach the lowest energy continuum state ($k = \infty$). This wavelength can be found from equation (5-20) to be

$$\lambda_n = \frac{hn^2}{E_R c}. \quad (5-28)$$

⁵The factor of λ^2/c in equation (5-25) results from the use of unit wavelength intervals instead of unit frequency intervals. In particular, in frequency terms, we would have $\alpha_\nu = \sigma_{nk} \frac{dk}{d\nu}$. As opacities are the fraction of a beam passing through the material that is removed from the beam, opacities must be identical in both frequency and wavelength formulations.

The bound free opacity at any wavelength can be found by adding the contributions due to all levels for which the wavelength is shorter than this cut-off wavelength. The lowest level from which bound-free absorption will occur is then

$$n_\lambda = \sqrt{\frac{E_R \lambda c}{h}}. \quad (5-29)$$

The opacity due to a level n will be given by the absorption cross-section for this level and the population per unit mass of hydrogen atoms in this state, so

$$\kappa_{n\lambda} = \alpha_{n\lambda} \frac{N_n}{\rho}. \quad (5-30)$$

In LTE, the population for a level n is given by equation (2-16)

$$\begin{aligned} N_n &= N_H \frac{g_n e^{-\chi_n/kT}}{U(T)} \\ &= N_H \frac{2n^2 e^{-\chi_n/kT}}{U(T)}. \end{aligned} \quad (5-31)$$

The total hydrogen bound-free opacity will then be given by

$$\kappa_{\text{H(bf)}} = \frac{2N_H}{\rho U(T)} \times 1.0435 \times 10^{-2} \lambda^3 \sum_{n=n_\lambda}^{\infty} \frac{e^{-\chi_n/kT} g_{\text{II}}(n, \lambda)}{n^3} \quad (5-32)$$

where $g_{\text{II}}(n, \lambda)$ is simply $g_{\text{II}}(n, k)$ with k given by equation (5-20). In practice, the sum cannot be calculated to $n = \infty$, but, since the photosphere of the sun is sufficiently cool so that most of the hydrogen is in the ground state, the highest states contribute very little so the sum of the lower bound states will give very nearly the same result. Alternately, the highest levels can be assumed to effectively form a continuum, and the sum can be treated as an integral for these highest states (usually assuming g_{II} to be 1).

A convenient approximation formula for g_{II} is given by Mihalas⁶:

$$g_{\text{II}}(n, x) = a_0 + a_1 x + a_2 x^2 + a_3 x^3 + a_{-1} x^{-1} + a_{-2} x^{-2} + a_{-3} x^{-3} \quad (5-33)$$

where $x = \frac{1}{\lambda}$, where λ is in microns. Table 5-1 below lists the constants a_i for the first ten levels.

⁶Pg 187 in Mihalas, D. "Statistical-Equilibrium Model Atmospheres for Early-Type Stars. I. Hydrogen Continua" *The Astrophysical Journal* **149**, pg 169-190 (1967).

Table 5-1: Coefficients in the Approximation Formula
for the Bound-Free Gaunt Factor⁷

n	a_0	a_1	a_2	a_3
1	1.2302628	$-2.9094219 \times 10^{-3}$	7.3993579×10^{-6}	$-8.7356966 \times 10^{-9}$
2	1.1595421	$-2.0735860 \times 10^{-3}$	2.7033384×10^{-6}	...
3	1.1450949	$-1.9366592 \times 10^{-3}$	2.3572356×10^{-6}	...
4	1.1306695	$-1.3482273 \times 10^{-3}$	$-4.6949424 \times 10^{-6}$	2.3548636×10^{-8}
5	1.1190904	$-1.0401085 \times 10^{-3}$	$-6.9943488 \times 10^{-6}$	2.8496742×10^{-8}
6	1.1168376	$-8.9466573 \times 10^{-4}$	$-8.8393113 \times 10^{-6}$	3.4696768×10^{-8}
7	1.1128632	$-7.4833260 \times 10^{-4}$	$-1.0244504 \times 10^{-5}$	3.8595771×10^{-8}
8	1.1093137	$-6.2619148 \times 10^{-4}$	$-1.1342068 \times 10^{-5}$	4.1477731×10^{-8}
9	1.1078717	$-5.4837392 \times 10^{-4}$	$-1.2157943 \times 10^{-5}$	4.3796716×10^{-8}
10	1.1052734	$-4.4341570 \times 10^{-4}$	$-1.3235905 \times 10^{-5}$	4.7003140×10^{-8}

n	a_{-1}	a_{-2}	a_{-3}
1	-5.5759888	1.2803223×10^1	...
2	-1.2709045	2.1325684	-2.0244141
3	-0.55936432	0.52461924	-0.23387146
4	-0.31190730	0.19683564	$-5.4418565 \times 10^{-2}$
5	-0.16051018	5.5545091×10^{-2}	$-8.9182854 \times 10^{-3}$
6	-0.13075417	4.1921183×10^{-2}	$-5.5303574 \times 10^{-3}$
7	$-9.5441161 \times 10^{-2}$	2.3350812×10^{-2}	$-2.2752881 \times 10^{-3}$
8	$-7.1010560 \times 10^{-2}$	1.3298411×10^{-2}	$-9.7200274 \times 10^{-4}$
9	$-5.6046560 \times 10^{-2}$	8.5139736×10^{-3}	$-4.9576163 \times 10^{-4}$
10	$-4.7326370 \times 10^{-2}$	6.1516856×10^{-3}	$-2.9467046 \times 10^{-4}$

This gives the gaunt factors to a good degree of accuracy for wavelengths down to about 50 Å, and is computationally much simpler than directly calculating them.

Figure 5-2 shows the hydrogen bound-free opacity.

⁷This table is from pg 187, Mihalas, D. "Statistical-Equilibrium Model Atmospheres for Early-Type Stars. I. Hydrogen Continua" *The Astrophysical Journal* **149**, pg 169-190 (1967).

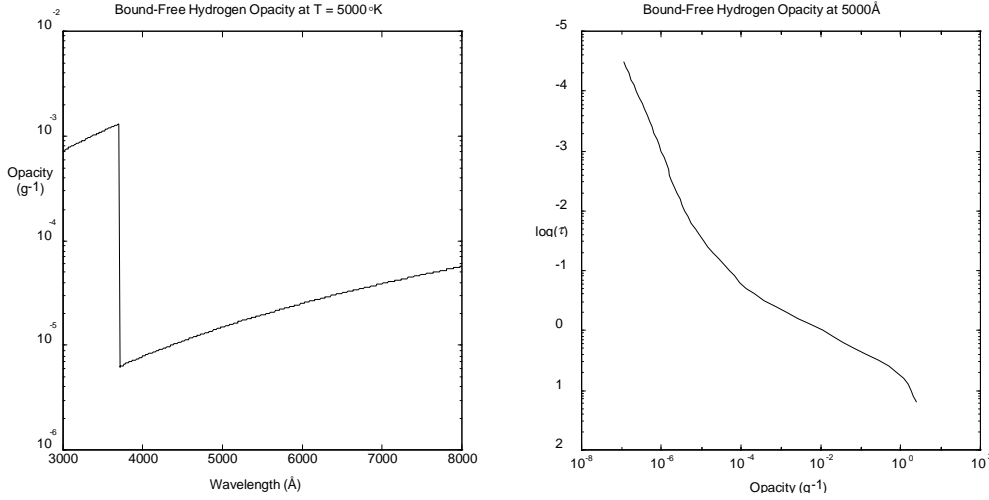


Figure 5-2: Hydrogen Bound-Free Opacity

5.3.3: Free-Free Hydrogen Opacity

The free-free opacity can be found in a similar manner. Both the initial and final states can be described by imaginary quantum numbers as defined by equation (5-19), so for a transition from a continuum state ik to il ,

$$\frac{hc}{\lambda} = E_R \left(\frac{1}{l^2} - \frac{1}{k^2} \right). \quad (5-34)$$

The oscillator strength for the transition can then be written in a form similar to equation (5-22),

$$f_{kl} = \frac{64}{3\pi\sqrt{3}} \frac{1}{g_k} \frac{1}{k^3 l^3} \left(\frac{1}{k^2} - \frac{1}{l^2} \right)^{-3} g_{\text{III}}(k, l) \quad (5-35)$$

where g_k is the multiplicity of the state ik as given in equation (2-19) which can be written in terms of k as

$$g_k = \frac{16\sqrt{2}\pi(m_e E_R)^{\frac{3}{2}}}{N_e h^3 k^4} dk. \quad (5-36)$$

The absorption cross-section for a single absorber is then

$$\alpha_{kl} = 1.0435 \times 10^{-2} \frac{2}{g_k} \frac{g_{\text{III}}(k, l)}{k^3} \lambda^3 \quad (5-37)$$

which is similar to the bound-free cross-section given in equation (5-27).

As the electrons have a Maxwellian velocity distribution, the population of absorbers per unit mass from a narrow band of states dk at a wavelength of λ is given by equation (2-17) as

$$\frac{N}{\rho} = \frac{N_{\text{H}}}{\rho} \frac{g_k e^{-E_R(1+1/k^2)/kT}}{U(T)}, \quad (5-38)$$

giving a total hydrogen free-free opacity of

$$\kappa_{\text{H(ff)}} = \frac{2N_{\text{H}}}{\rho U(T)} \times 1.0435 \times 10^{-2} \lambda^3 \int_0^{\infty} \frac{e^{-E_R(1+1/k^2)/kT}}{k^3} g_{\text{III}}(k, \lambda) dk \quad (5-39)$$

The integral can be readily done if the Gaunt factor $g_{\text{III}}(k, \lambda)$ is replaced by a suitable thermal average Gaunt factor $g_{\text{III}}(\lambda, T)$ giving

$$\kappa_{\text{H(ff)}} = \frac{2N_{\text{H}}}{\rho U(T)} \times 1.0435 \times 10^{-2} \lambda^3 \frac{e^{-E_R/kT}}{2 E_R/kT} g_{\text{III}}(\lambda, T). \quad (5-40)$$

A convenient formula for g_{III} is given by Mihalas⁸:

$$\begin{aligned} g_{\text{III}}(x, \theta) \approx & (1.070192 + 3.9999187 \times 10^{-3}/\theta - 7.8622889 \times 10^{-5}/\theta^2) \\ & + (0.26061249 + 6.4628601 \times 10^{-2}/\theta - 6.1953813 \times 10^{-4}/\theta^2)/x \\ & + (-0.57917786 - 3.7542343 \times 10^{-2}/\theta - 1.3983474 \times 10^{-5}/\theta^2)/x^2 \\ & + (0.34169006 + 1.1852264 \times 10^{-2}/\theta)/x^3 \end{aligned} \quad (5-41)$$

where $x = \frac{1}{\lambda}$, where λ is in microns, and $\theta = \frac{5040^\circ \text{K}}{T}$.

The free-free hydrogen opacity is shown in figure 5-3.

⁸Pg 187 in Mihalas, D. "Statistical-Equilibrium Model Atmospheres for Early-Type Stars. I. Hydrogen Continua" *The Astrophysical Journal* **149**, pg 169-190 (1967). For wavelengths greater than 10 000 Å, the following formula (also from Mihalas as above) is suitable:

$$g_{\text{III}} \approx (1.0823 + 0.0298/\theta) + (0.0067 + 0.0112/\theta)/x. \quad (5-41B)$$

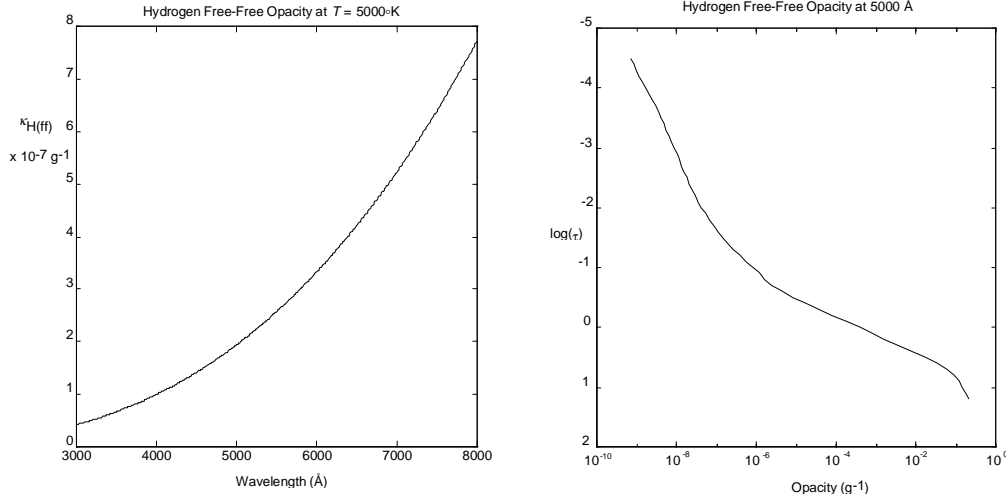


Figure 5-3: Hydrogen Free-Free Opacity

The total opacity due to atomic hydrogen can readily be found by using equations (5-32) and (5-40), so

$$\begin{aligned} \kappa_{\text{H}} &= \frac{2N_{\text{H}}}{\rho U(T)} \times 1.0435 \times 10^{-2} \lambda^3 e^{-E_{\text{R}}/kT} \left(\sum_{n=n_{\lambda}}^{\infty} \frac{e^{(E_{\text{R}}-\chi_n)/kT} g_{\text{II}}(n, \lambda)}{n^3} + \frac{g_{\text{III}}(\lambda, T)}{2E_{\text{R}}/kT} \right) \\ &= \frac{N_0}{\rho} \times 1.0435 \times 10^{-2} \lambda^3 e^{-E_{\text{R}}/kT} \left(\sum_{n=n_{\lambda}}^{\infty} \frac{e^{(E_{\text{R}}-\chi_n)/kT} g_{\text{II}}(n, \lambda)}{n^3} + \frac{g_{\text{III}}(\lambda, T)}{2E_{\text{R}}/kT} \right) \end{aligned} \quad (5-42)$$

where N_0 is the number density of atomic hydrogen in the ground state. As stimulated emission has not yet been accounted for, the usual correction for stimulated emission must still be made, so the opacity will be

$$\begin{aligned} \kappa_{\text{H}} &= \frac{N_0}{\rho} \times 1.0435 \times 10^{-2} \lambda^3 e^{-E_{\text{R}}/kT} (1 - e^{-hc/\lambda kT}) \\ &\quad \times \left(\sum_{n=n_{\lambda}}^{\infty} \frac{e^{(E_{\text{R}}-\chi_n)/kT} g_{\text{II}}(n, \lambda)}{n^3} + \frac{g_{\text{III}}(\lambda, T)}{2E_{\text{R}}/kT} \right) \end{aligned} \quad (5-43)$$

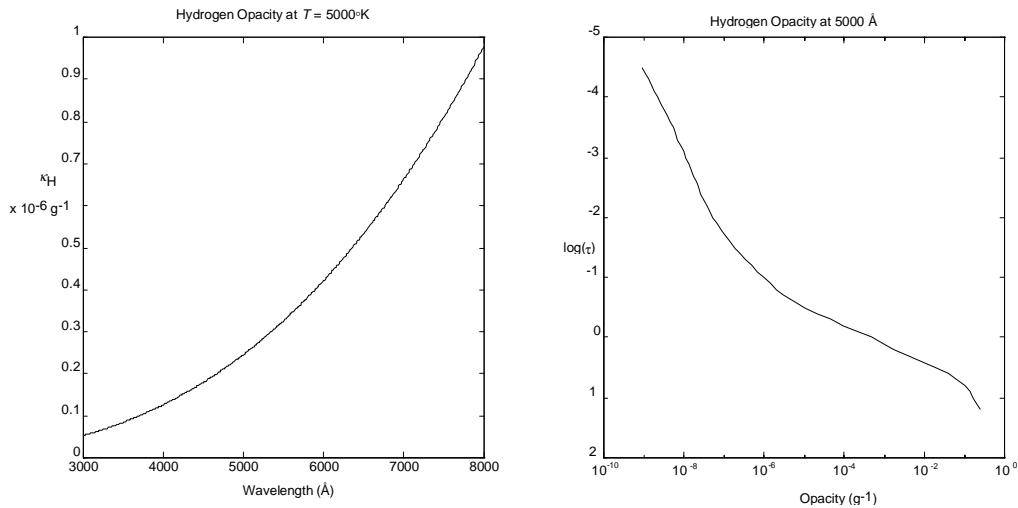


Figure 5-4: Hydrogen Opacity

5.3.4: H_2^+ Molecule Opacity

The H_2^+ molecule is a reasonably important absorber in the solar photosphere. Like all complex absorbers, the calculation of the absorption cross-section is rather more difficult than for atomic hydrogen. Cross-sections for H_2^+ have been calculated⁹, so these results can be used, with intermediate values being interpolated.¹⁰ The H_2^+ opacity is shown in figure 5-5.

⁹For example, by Bates in Bates, D.R. "Absorption of Radiation by an Atmosphere of H, H^+ and H_2^+ - Semi-Classical Treatment" *Monthly Notices of the Royal Astronomical Society* **112**, pg 40-44 (1952) and by Buckingham et al. in Buckingham, R.A., Reid, S. and Spence, R. "Continuous Absorption by the Hydrogen Molecular Ion" *Monthly Notices of the Royal Astronomical Society* **112**, pg 382-386 (1952).

¹⁰A convenient tabulation is that given by Matsushima in Harvard-Smithsonian Conference on Stellar Atmospheres "Proceedings of the First Conference" *Smithsonian Astrophysical Observatory Special Report* **167**, Smithsonian Astrophysical Observatory, Cambridge (1964).

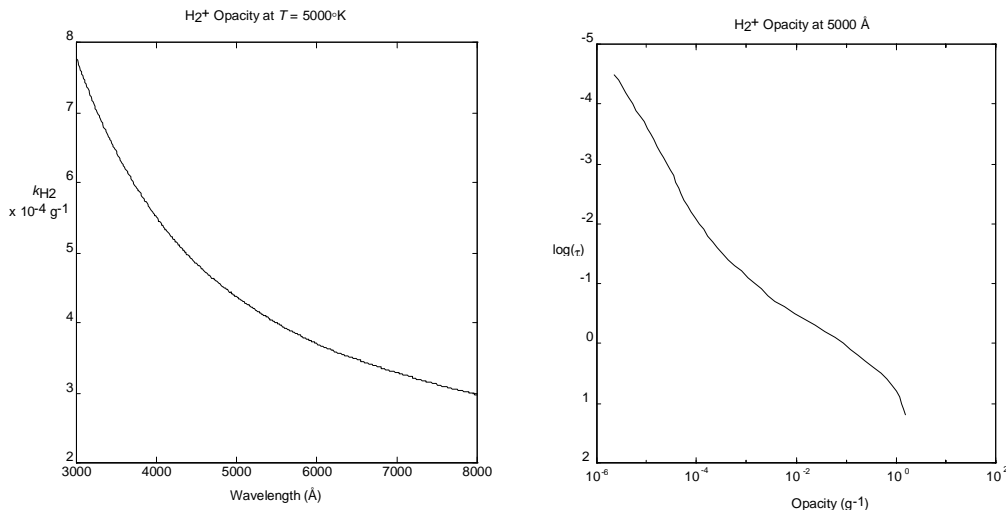


Figure 5-5: H_2^+ Opacity

5.3.5: Opacity Due to Heavier Elements

As their abundances are much lower than hydrogen, heavier elements make correspondingly smaller contributions to the total opacity. Most heavy elements have lower ionisation energies than hydrogen, so photoionisation of such elements can be important at wavelengths short enough to ionise such elements but long enough so that hydrogen photoionisation is negligible. Free-free processes will also contribute to the total opacity. Calculations for such processes cannot be performed exactly as heavy atoms are excessively complex systems.

Approximate solutions can be obtained by using suitable approximate wave functions for the atomic system. The calculations can then be done in a manner similar to that for hydrogen. Only the most abundant atomic species need be considered, and then only those that make an appreciable contribution to the total opacity need to be taken into account. Calculations in reasonable agreement with experimental results were made by Peach for a number of important elements (C, N, O, Mg, Mg II, Si, Cl and Ca II).¹¹ The opacities due to magnesium and silicon (the most important of the

¹¹Peach, G. "Total Continuous Absorption Coefficients for Complex Atoms" *Memoirs of the Royal Astronomical Society* **71**, pg 29-45 (1967).

heavy elements contributing to the continuous opacity of the solar photosphere in the visible spectrum) are shown in figures 5-6 and 5-7.

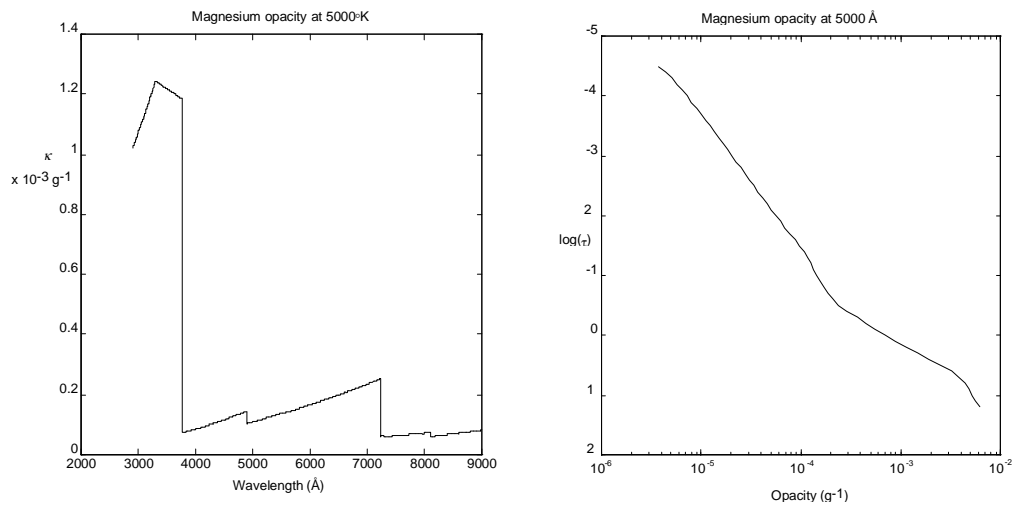


Figure 5-6: Mg Opacity

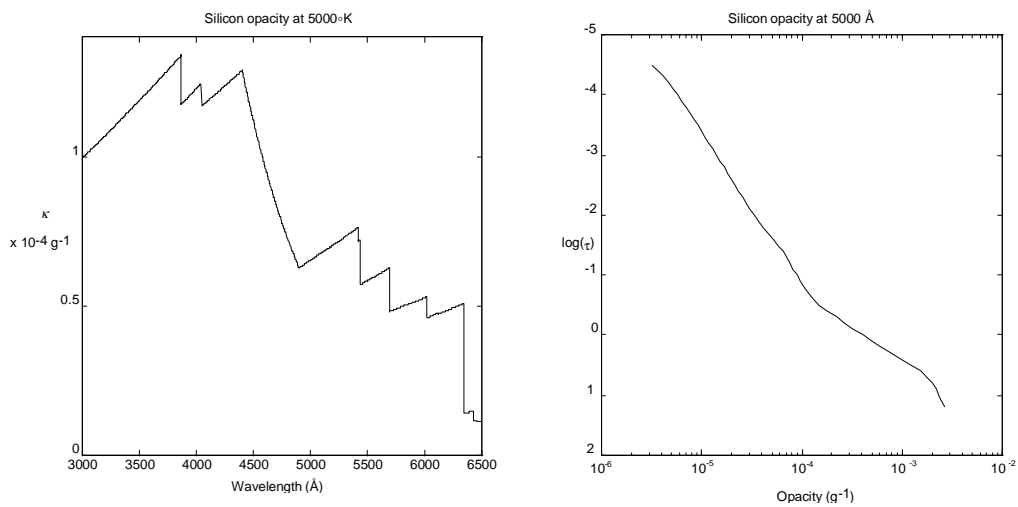


Figure 5-7: Si Opacity

5.3.6: Other Sources of Opacity

Other sources of opacity do not need to be considered for the visible region of the solar spectrum. Solar photospheric scattering was shown to be negligible in chapter 3 (see table 3-1 and table 3-2) but might need to be considered for other stars, or for other regions of the solar spectrum.

Due to its abundance, helium can be important in some stars, but because the lowest excited state of helium has a high excitation energy (19.72 eV), helium opacity at visible wavelengths will be significant only for hot stars.¹² If the star is hot enough, ionised helium can also contribute to the opacity. For cool stars, the negative helium ion He^- can contribute to the free-free opacity. None of these processes are important in the solar photosphere.¹³

The most important contributions to the continuous opacity of the photosphere are shown in figure 5-8. It can be readily seen that the major contribution is due to the H^- ion, with other sources of opacity only being important deep in the photosphere, or in the ultraviolet spectrum.

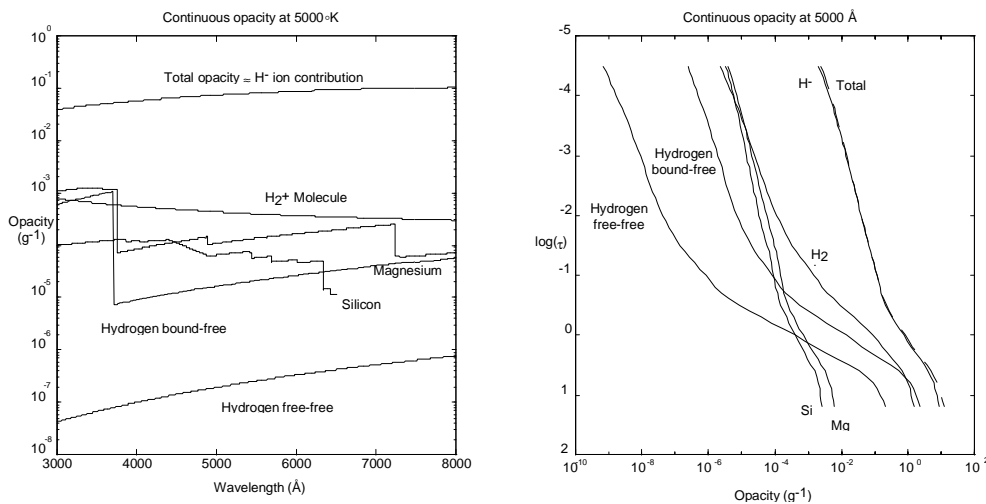


Figure 5-8: Contributions to Continuous Opacity

¹²Helium can dominate the opacity in some stars where the helium abundance is extremely high (such as when it is comparable to the hydrogen abundance).

¹³See Mihalas, D. "Stellar Atmospheres" Freeman, San Francisco (1970) pg 120-123 for a discussion of helium opacity.

5.4: Line Opacities

Calculation of line opacities involves finding the opacities at all wavelengths of interest for all lines in the spectral region being calculated. The opacity due to a spectral line is given by equation (3-46)

$$\kappa_{\lambda} = \frac{N}{\rho} \frac{\pi e^2}{m_e c} g f \frac{e^{-hc/\lambda kT}}{U(T)} (1 - e^{-hc/\lambda kT}) \phi(\lambda). \quad (5-44)$$

This expression consists of a line strength dependent on the transition oscillator strength and the population of the lower level of the transition, a correction for stimulated emission (where stimulated emission is treated as negative absorption), and the line profile function. The level population and stimulated emission correction factor given here are only valid in LTE, but a similar formulation would be used in NLTE cases.

The correction factor for stimulated emission is the simplest to deal with; it is dependent only on the wavelength (effectively constant across the entire spectral line) and the local temperature. The line strength and the line profile function present more difficulty.

5.4.1: The Line Strength

The line strength depends on the population of the lower level of the transition and the oscillator strength. In LTE, the level population is given by equation (2-16)

$$N_i = N \frac{g_i e^{-E_i/kT}}{U(T)} \quad (5-45)$$

where N is the number density of the atom in the correct ionisation state. The fraction of the total population of the atom in this ionisation state can be found by using Saha's equation (equation (2-21)).

The calculation of the partition function $U(T)$ can be difficult. If values for the partition function are known at some temperatures, intermediate values can be found by interpolation, or a suitable approximation formula for the partition function can be used.

The multiplicity of the state g_i is usually combined with the oscillator strength as a gf-value. Accurate calculation of the gf-value is, in general, not feasible as part of a spectral synthesis process¹⁴, so it is necessary to use gf-values from other sources. Although some gf-values can be calculated to reasonable degree of accuracy, for most transitions, it will be necessary to use more accurate experimental results.

For the purpose of investigating line profiles, if a gf-value is not known sufficiently accurately, a suitable value can be chosen so as to give a good fit between the observed and calculated spectra. If this is done, it reduces the information available from the spectrum (if the gf-value is known, the abundance of the element in the photosphere can be determined, or, if both the abundance and gf-value are well known, values obtained for other line parameters such as damping are correspondingly more reliable), but this is often unavoidable.

Calculations, such as those used to fit model atmospheres, that involve large regions of the spectrum and thus contain many lines require large numbers of gf-values, although if no lines are examined in detail, data of lower accuracy is sufficient as long as there are no systematic errors.

In general, there is a need for more, and more accurate, gf-values.¹⁵

5.4.2: The Line Profile

The line profile function depends on the small-scale velocity fields (see sections 3.5 and 3.6) and on the damping of the transition (see Chapter 4: Damping). The small-scale velocity field consists of thermal motions and of small-scale mass motions. Both must be taken into account.

Thermal motions cause no great difficulty. The absorber velocity distribution is Maxwellian (even for NLTE cases)¹⁶ so the thermal contribution to the line profile

¹⁴See Appendix A for information on the calculability and measurability of gf-values.

¹⁵For many transitions, accurate data are available. Appendix A discusses various sources of gf-values. Often, however, an accurate value is not available for a particular transition, necessitating either using less accurate data or experimentally obtaining a gf-value for the transition. See Appendix B: An Automated Spectrometer for a discussion of an experiment to measure gf-values.

function is to give a Voigt profile instead of the stationary atom Lorentz profile. The Voigt profile is given by equation (3-71)

$$\begin{aligned}\phi_D(\lambda) &= U(a, \nu) \\ &= \frac{a}{\pi^{\frac{3}{2}}} \int_{-\infty}^{\infty} \frac{e^{-x^2}}{(\nu-x)^2 + a^2} dx \\ &= \frac{1}{\sqrt{\pi}} H(a, \nu)\end{aligned}\quad (5-46)$$

where ν is the number of Doppler widths that the wavelength is away from the line centre, and a is the ratio of the Lorentzian profile half-width to the Doppler full-width.

The number of Doppler widths from line centre ν is given by

$$\nu = \frac{\lambda - \lambda_0}{\Delta\lambda_D} \quad (5-47)$$

where $\Delta\lambda_D$ is the Doppler half-width, given by

$$\Delta\lambda_D = \frac{\lambda_0}{c} \sqrt{\frac{2kT}{m}}. \quad (5-48)$$

The ratio of the Lorentzian profile width to the Doppler width a is then

$$a = \frac{\Delta\lambda_L}{2\Delta\lambda_D}. \quad (5-49)$$

As mentioned in section 3.5, there are simple approximate methods by which the Voigt function can be calculated for large ν and a . For the case where a is small (of great interest for photospheric lines as the Lorentzian profile width is usually quite small compared to the Doppler width), the Voigt function can be replaced by a power series in terms of a such as:

$$H(a, \nu) = \sum_{n=0}^{\infty} H_n(\nu) a^n. \quad (5-50)$$

The coefficients H_n are¹⁷

$$H_n(\nu) = \frac{(-1)^n}{\sqrt{\pi n!}} \int_0^{\infty} e^{-x^2/4} x^n \cos \nu x dx. \quad (5-51)$$

¹⁶In the photosphere. For other cases where collisions become rare, such as nebulae, or the corona, this will not be the case.

¹⁷See Mihalas, D. "Stellar Atmospheres", Freeman (1970) for the details of the derivation of this series.

The values of the first few coefficients are shown in table 5-2, with the odd coefficient in terms of $Q(v)$, where

$$Q(v) = 1 - 2vF(v) \quad (5-52)$$

where **Dawson's function** $F(v)$ is defined by

$$F(v) = e^{-v^2} \int_0^v e^{t^2} dt. \quad (5-53)$$

Table 5-2: Coefficients in Voigt Function Power Series

n	$H_n(v)$
0	e^{-v^2}
1	$\frac{-2}{\sqrt{\pi}} Q(v)$
2	$(1 - 2v^2)e^{-v^2}$
3	$\frac{-2}{\sqrt{\pi}} \left(-\frac{1}{3} + \left(1 - \frac{2}{3}v^2\right) Q(v) \right)$
4	$\left(\frac{1}{2} - 2v^2 + \frac{2}{3}v^4 \right) e^{-v^2}$
5	$\frac{-2}{\sqrt{\pi}} \left(-\frac{7}{30} + \frac{4}{30}v^2 + \left(\frac{1}{2} - \frac{4}{3}v^2 + \frac{16}{30}v^4 \right) Q(v) \right)$
6	$\left(\frac{1}{6} - v^2 + \frac{2}{3}v^4 - \frac{4}{45}v^6 \right) e^{-v^2}$

Provided a is sufficiently small (say, less than 0.6), these coefficients can be used to readily calculate the Voigt function, given a suitable method to calculate Dawson's function. Dawson's function can be approximately found by numerical integration at suitable points, and then either interpolating from these values or using them to construct a piecewise polynomial fit to Dawson's function. Dawson's function approximated as a ninth-order polynomial (in v^2 , v , and v^{-2}) is shown in table 5-3.

Table 5-3: Polynomial Fit to Dawson's Function¹⁸

$a_n v^n$	$(v^2)^n, 0 < v < 1$	$v^n, 1 < v < 2$	$(v^{-2})^n, 2 < v < 5$
a_0	1.00000	-0.22320	0.50020
a_1	-0.66666	1.5540	0.24180
a_2	0.26664	-3.7803	0.11409
a_3	-7.6123×10^{-2}	8.4897	22.935
a_4	1.6834×10^{-2}	-10.172	-5.3695×10^2
a_5	-2.9935×10^{-3}	6.8149	6.5782×10^3
a_6	4.2629×10^{-4}	-2.7004	-4.2740×10^4
a_7	-4.5898×10^{-5}	0.63121	1.5176×10^5
a_8	3.2685×10^{-6}	-8.0278×10^{-2}	-2.8190×10^5
a_9	-1.1267×10^{-7}	4.2446×10^{-3}	2.1578×10^5

For large values of a or v , the Voigt function asymptotically approaches the Lorentz function. This can be used to obtain approximation formulae suitable for rapidly calculating the Voigt profile. These cases are less important for the cases examined in this work, as the line profile function becomes very small at moderate distances from the line centre (i.e. at large v), and a tends to be quite small.

For cases not covered by these approximation formulae, it is necessary to numerically integrate equation (5-46).

An alternative technique is to simply find the Lorentzian damping profile and the Gaussian Doppler profile, both of which can be found readily, and numerically find their convolution, thus obtaining the Voigt profile.

¹⁸The fits for $v < 1$ and $v > 2$ are from Ross, J.E.R. "Syn - FORTRAN Spectral Synthesis Program for MS-DOS" Physics Department, The University of Queensland (1995).

5.5: Damping

The most important contribution to damping is collisions with neutral hydrogen (almost all of which is in the ground state). As an accurate treatment is desirable, the Brueckner-O'Mara theory can be used to compute damping constants due to such collisions.¹⁹ This involves finding the two damping parameters σ and α for each transition. The resultant damping can then be found using equations (4-54) and (4-53). As shown in table 4-5, other contributions to the damping will be significantly smaller. Accurate results were available only for s-p and p-s transitions. Other damping constants were estimates only, and fitting the observed and computed spectra was necessary to determine them more accurately.

Other sources of broadening are much less important. The damping due to electrons is over an order of magnitude less than the damping due to neutral hydrogen in the regions of the photosphere where spectral lines form. (At $\tau_{5000\text{\AA}} = 1$, it is 50 times smaller, and becomes even less important with increasing height.)

Broadening by collisions with neutral helium are also much less important. Due to the higher mass and consequent lower velocity of helium atoms, along with the smaller electric fields (due to the more symmetric distribution of electrons) associated with helium atoms, and the lower helium abundance, the damping due to helium is about 30 times smaller than that due to hydrogen.

Minor sources of impact broadening, such as ions and other neutral atoms can be safely neglected, particularly in view of the relatively large uncertainties in the major contributions to the total damping. Errors in computing the damping of a transition are likely to be some of the largest errors in calculating synthetic spectra.

Under different conditions, such as atmospheres in which the degree of ionisation is greater, or in which excited hydrogen atoms are more important, will require a somewhat different approach, so as to deal with the most important sources of damping most accurately.

¹⁹See Anstee, S.D. and O'Mara, B.J. "Width Cross-Sections for Collisional Broadening of s-p and p-s Transitions by Atomic Hydrogen" *Monthly Notices of the Royal Astronomical Society* **276**, pg 859-866 (1995). An early version of these results was supplied by J.E. Ross and B. O'Mara.

5.6: Velocity Fields

Mass motions will affect the line profile function, and are readily seen to have a major effect as they must be included in order to obtain even a rough fit between observed and calculated spectral lines in most cases. The standard simple treatment of mass motions is to divide them into small-scale motions, called microturbulence, and large-scale motions, called macroturbulence. To extend this treatment generally requires going beyond a simple plane-parallel analysis.

5.6.1: The Standard Model - Macro- and Microturbulence

The standard treatment of mass motions is to divide them into microturbulent motions, which are small compared to the photon mean free path, and in a plane-parallel atmosphere, are small compared to the stratification, and macroturbulent motions, which are large-scale motions.

Macroturbulence is a simple extension of a purely plane-parallel atmosphere in order to take (non-homogeneous) large-scale motions into account. If we consider one of a great number of elements of a plane-parallel atmosphere, each with a uniform line-of-sight velocity, the line profile function will not change shape but will merely be shifted in wavelength by the motion. Such motions will therefore cause broadening of the emergent spectrum.

This broadening can be found by convoluting the emergent spectrum from a macroscopically stationary atmosphere with the distribution of Doppler shifts due to the macroturbulence. The macroturbulent motions are assumed to have a Gaussian distribution.

The velocity distribution due to a macroturbulent velocity Ξ is

$$W(v)dv = \frac{1}{\Xi\sqrt{\pi}} e^{-v^2/\Xi^2} dv, \quad (5-54)$$

which gives a Doppler shift distribution in the vicinity of a spectral line of wavelength λ_0 of

$$W(\Delta\lambda)d\Delta\lambda = \frac{1}{\Delta\lambda_0\sqrt{\pi}} e^{-(\Delta\lambda)^2/(\Delta\lambda_0)^2} d\Delta\lambda \quad (5-55)$$

where the most probable shift $\Delta\lambda_0$ is given by

$$\Delta\lambda_0 = \frac{\Xi}{c} \lambda_0. \quad (5-56)$$

The convolution of this Doppler shift distribution with the macroscopically stationary emergent spectrum gives the observed spectrum.

The microturbulence is also assumed to have a Gaussian distribution. A Gaussian, or very nearly so, velocity distribution is expected for small scale turbulence. The Gaussian distribution from microturbulent motions simply increases the width of the Gaussian Doppler profile already present due to thermal motions. The new Doppler width is simply

$$\Delta\lambda_D = \frac{\lambda_0}{c} \sqrt{\frac{2kT}{m} + \xi_{\text{turb}}^2} \quad (5-57)$$

where ξ_{turb} is the microturbulence (the most probable line-of-sight microturbulent velocity). As a purely plane-parallel atmosphere is assumed, the microturbulence is assumed to be horizontally uniform.

Microturbulence thus acts in a manner similar to thermal motions. The microturbulence, unlike the thermal motions, does not depend on the atomic mass of the absorber. This gives a way in which they can be distinguished. The macroturbulence, affecting only the emergent spectrum as a whole, has no effect on the equivalent widths of spectral lines; it only serves to broaden the profiles. Microturbulence, on the other hand, will affect the equivalent width as it will affect the line opacity. This effect on equivalent widths can be quite pronounced for strong lines. For weak lines, for which the intensity is almost independent of wavelength, the effect on the equivalent width is much smaller.

This treatment has the advantage of being simple, and if an exact fit to the shape of the spectral line is not necessary, can be quite adequate, such as when abundances from weak lines are being found. It fails to provide any source of asymmetry, and thus must fall short of reality in at least some respects.

5.6.2: The Standard Model - Common Variants

While microturbulence is frequently assumed to be independent of depth (as a simplification, and to reduce the number of free parameters), depth dependent microturbulence can be assumed within the plane-parallel framework.

Macroturbulence is also occasionally assumed to be depth dependent, but this can only be done in a plane-parallel framework by assuming that the entire horizontal stratum has some mean vertical velocity, and that the variation about this vertical velocity is independent of depth although the mean velocity varies with depth.²⁰ While this can be a convenient technique, it cannot accurately model the reality of the photospheric large-scale motions.

5.6.3: Beyond Macroturbulence

Gaussian macroturbulence, while a convenient assumption, is not representative of photospheric mass motions. Large scale mass motions in the photosphere are asymmetric and non-Gaussian, so the standard use of macroturbulence must be modified. Photospheric mass motions also vary with depth within the photosphere, while the simple macroturbulence theory assumed depth-independent motions. Modifications of the treatment of macroturbulence required to better represent photospheric motions are explored in greater depth in chapters 7 and 8.

5.6.4: Granulation and Realistic Microturbulence

While it may be possible to treat realistic macroturbulence as plane-parallel (but only if the depth dependence of the macroturbulence is small), attempts to treat microturbulence in a realistic manner violate the plane-parallel formulation, as observations of granulation clearly show that microturbulence is not horizontally

²⁰See, for example, Stathopoulou, M. and Alissandrakis, C.E. "A Study of the Asymmetry of Fe I Lines in the Solar Spectrum" *Astronomy and Astrophysics* **274**, pg 555-562 (1993).

uniform. Thus, it will not be possible to exactly calculate spectra taking granulation into account without abandoning the plane-parallel approximation. Some useful results will be obtainable by assuming a suitable average microturbulence and proceeding as before, but to adequately examine line profiles and the effect of granulation upon them, it is necessary to use non-plane-parallel spectral synthesis. The starting point for such an approach is still the plane-parallel case, as the non-plane-parallel case is most simply dealt with as a collection of plane-parallel regions, each which can be dealt with as described below.

5.7: Spectral Synthesis

5.7.1: Spectral Synthesis Software

The preceding sections of this chapter covered the basic principles of spectral synthesis. This can be used to gain an insight into spectral synthesis; knowing what goes into such a process can help one understand what can be obtained from it. It can also be used as a recipe for developing a spectral synthesis program. LTE spectral synthesis can be performed quite adequately on modern microcomputers, and there are already many spectral synthesis programs already written for microcomputers.

The development of such a spectral synthesis program is simply the implementation of the technique described in this chapter. The heart of a spectral synthesis program is simply a numerical integration routine, with the opacity calculations necessary being supplied to this routine.

The radiative transfer equation for the photosphere, with the source function being a monotonically increasing function of optical depth, is well behaved provided it is solved in a reasonably robust manner. If it is solved in an inappropriate manner, small errors can grow exponentially until they destroy any useful results which might otherwise be obtained. A suitable method is to integrate

$$I_{\lambda}(\tau = 0) = \int_0^{\infty} S_{\lambda}(\tau_{\lambda}) e^{-\tau_{\lambda}/\mu} \frac{1}{\mu} d\tau_{\lambda}. \quad (5-58)$$

Model atmospheres are generally given as a tabulation of atmospheric parameters at various optical depths at a particular wavelength (usually 5000Å, but other

wavelengths such as 4000\AA are occasionally used). The optical depths are usually given with a uniform logarithmic interval, so the atmosphere is divided into strata of constant thickness $d(\log \tau_0)$, thus determining the points available for the numerical integration of equation (5-58). As the points τ_λ for the integration are determined by the model atmosphere, there is less value in using Gaussian quadrature integration than if we could choose them freely. Equation (5-58) can only be integrated from the uppermost layer given in the model atmosphere to the lowest, but as long as any spectral lines in the spectral region of interest originate in the photosphere, and the entire photosphere is included in the model atmosphere, contributions from other portions of the atmosphere will be negligible.

It is generally convenient to use uniformly spaced wavelength points. Uniformly spaced points mean that the wavelength points to use can be the same at all optical depths and can be determined beforehand. A non-uniform distribution of wavelength points could be useful, with a higher density of points being used where opacities or the intensity change more rapidly, and a lower density of points where they change more slowly. Thus, a large spectral region could be represented by the minimum number of points needed to convey the information accurately. It would mean, however, having some knowledge of the opacity and intensity before choosing a final set of wavelength points.

As solar spectra are usually given as functions of wavelength rather than frequency, if comparisons between observed and calculated spectra are desired, it is convenient to calculate the emergent spectrum as a function of wavelength (thus the use of wavelength rather than frequency throughout this work). The spacing of wavelength points can also be chosen to be the same as the spectral data used, or some multiple thereof, so as to make comparison easier.

5.8: Results of Plane-Parallel LTE Spectral Synthesis

5.8.1: Use of Plane-Parallel Spectral Synthesis

Plane-parallel spectral synthesis was carried out for the lines being examined in this work. This is a reliable technique to check the accuracy of transition parameters and adjust them where necessary. This is likely to prove necessary, as the oscillator strengths for many of the lines are not well known, and the accuracy of the damping parameters used for the lines should also be examined, and the values adjusted if necessary.

Performing a standard plane-parallel spectral synthesis analysis of the lines studied also enables the closeness of the best fit obtainable using this method to be compared quantitatively with the closeness of fit obtainable using a non-plane-parallel spectral synthesis method as performed in chapter 8 (see section 8.3.5 for such a comparison).

Much of this involves calculating a synthetic spectrum, and comparing it to the observed solar line. New estimates of any required parameters can then be obtained, and a new spectrum calculated, and in this way, the fit between the observed and computed spectra can be steadily improved. The results of this process are discussed in detail in section 5.8.3.

5.8.2: Quality of Synthesised Profiles

As expected, the main deviation between the observed and calculated spectra is due to the asymmetry of the observed lines (and the symmetry of the synthetic line profiles). As the asymmetry of the line profiles is generally small, the fits between the observed and calculated spectra are quite good. A selection of plane-parallel synthetic spectra are shown in figures 5-9, 5-10, 5-11, 5-12 and 5-13.

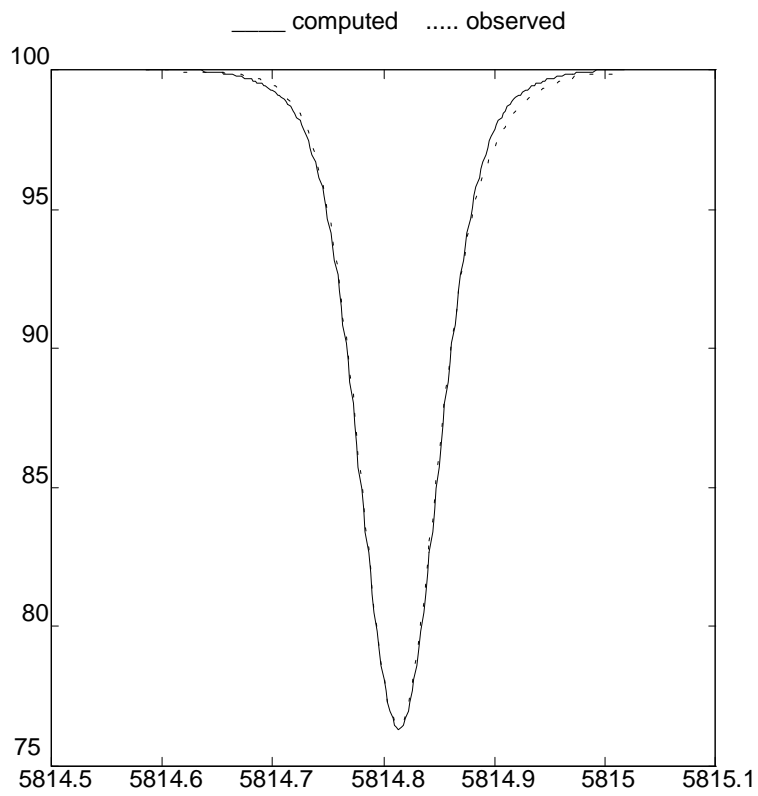


Figure 5-9: Fe I at 5814.814Å

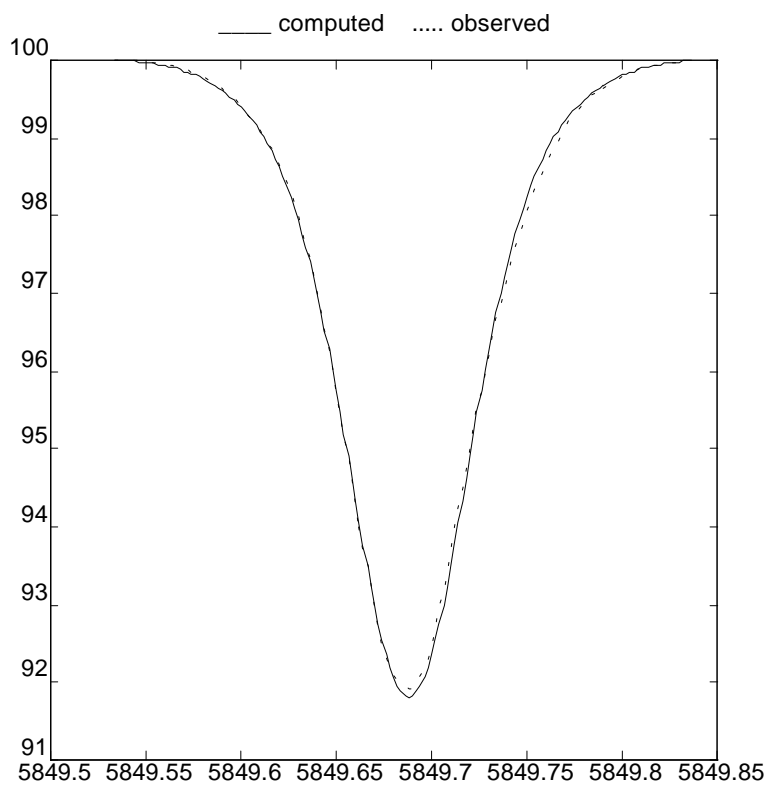


Figure 5-10: Fe I at 5849.687Å

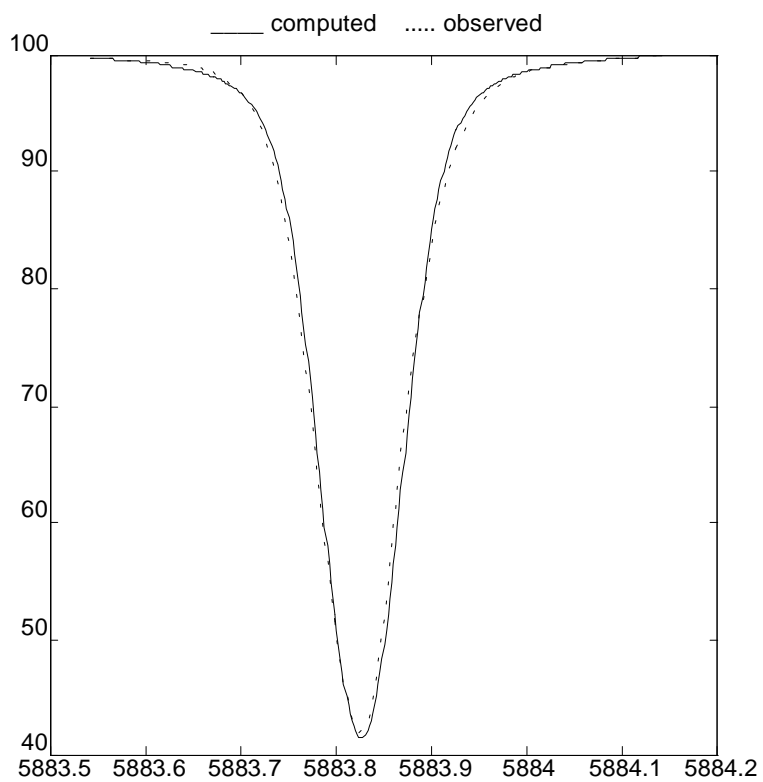


Figure 5-11: Fe I at 5883.823 Å

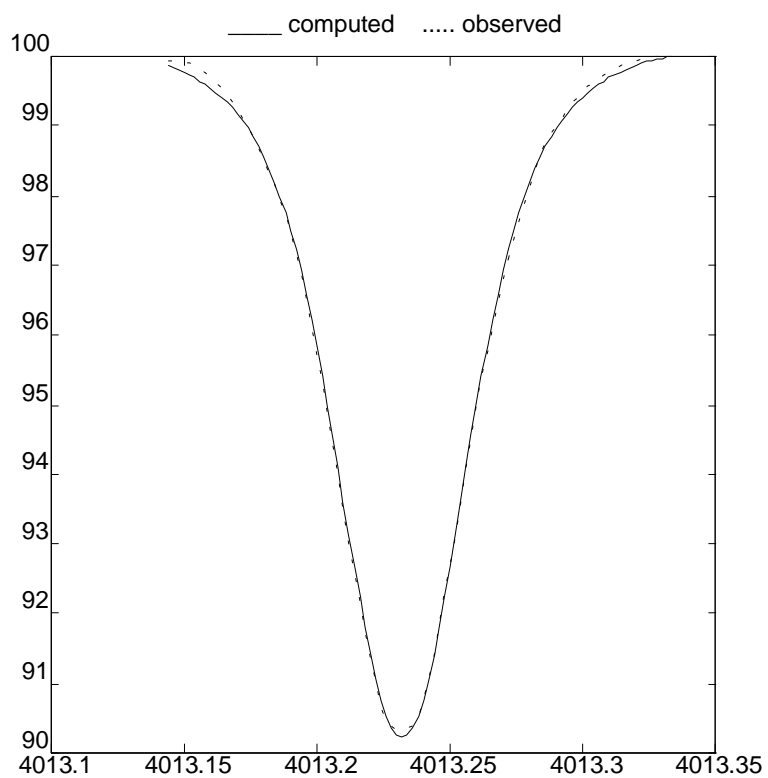


Figure 5-12: Ti I at 4013.232 Å

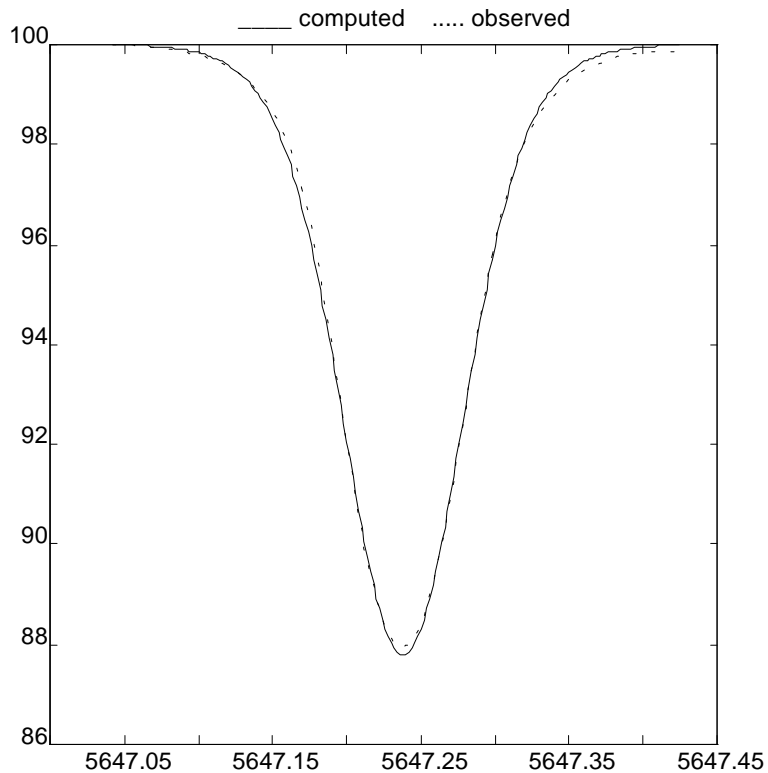


Figure 5-13: Co I at 5647.238Å

It is readily seen that it is impossible to fit both the red and blue wings of the observed and computed profiles simultaneously. In order to fit the profiles better, a departure from the plane-parallel atmosphere must be made. Non-plane-parallel spectral synthesis is examined in chapter 8. Such calculations, fitting observed profiles more closely, can give better results for determinations of line and atmospheric parameters from the observed spectrum. See section 8.3.5 for a comparison between the best fits obtainable using the standard plane-parallel technique and non-plane-parallel spectral synthesis.

5.8.3: Determination of Parameters

A limited amount of information can be extracted from the solar spectrum using plane-parallel spectral synthesis. A number of parameters of both the atomic transition giving rise to the absorption line involved and the model atmosphere affect the line profile. The strongest effect is that of the abundance of the element (an

atmospheric parameter) and the oscillator strength or f -value of the line on the total strength of the line. The equivalent width of the line is strongly affected by the product of these parameters (or sum if expressed logarithmically). A reasonable estimate of this product can thus be obtained from the equivalent width alone, without recourse to detailed matching of profiles. The equivalent width is also affected by the broadening of the line, particularly for strong lines.²¹ Thus, a result obtained using line profiles should be more accurate than a method using equivalent widths alone.

Data on broadening processes can also be obtained, but this can be quite uncertain, particularly in view of the discrepancies between the actual photosphere and any plane-parallel model thereof.

In view of the large number of lines examined, and the possibility of therefore determining a number of solar abundances to a reasonable degree of accuracy, even without particularly accurate oscillator strengths for many of the lines, the photospheric abundance of each element required for each individual line was found, rather than adjusting the gf -values of the lines. The mean of these values can then be found to determine a photospheric abundance of the appropriate elements. As a small number of the lines examined did not have known oscillator strengths, these were obtained from such fits. These lines were excluded from the abundance analysis.

A similar abundance analysis using non-plane-parallel spectral synthesis is presented in section 8.3.6.

²¹The basic distinction between strong lines and weak lines is that weak lines have equivalent widths unaffected by broadening processes, while the equivalent widths of strong lines are affected. This is a function of the degree of saturation of the line.

Table 5-4: Photospheric Abundances

Element	Lines	Abundance	Standard Solar	Meteoric
Si	2	6.80	7.55 ± 0.05	7.55 ± 0.02
K	1	5.49	5.12 ± 0.13	5.13 ± 0.03
Ti	15	5.02 ± 0.12	4.99 ± 0.02	4.93 ± 0.02
V	7	4.10 ± 0.08	4.00 ± 0.02	4.02 ± 0.02
Cr	9	5.77 ± 0.10	5.67 ± 0.03	5.68 ± 0.03
Mn	1	5.48	5.39 ± 0.03	5.53 ± 0.04
Fe	63	7.62 ± 0.04	7.67 ± 0.03	7.51 ± 0.01
Co	5	4.76 ± 0.05	4.92 ± 0.04	4.91 ± 0.03
Ni	17	6.30 ± 0.14	6.25 ± 0.04	6.25 ± 0.02
Mo	1	1.94	1.92 ± 0.05	1.96 ± 0.02

The abundances obtained from the lines examined are in good agreement with the expected results. The only elements with large deviations are silicon and cobalt. Only two silicon lines were available, and only five cobalt lines, so errors in the oscillator strengths will be very important. The abundances of elements for which more lines were available are more reliable, and better agreement with accepted values was obtained. It can also be noted that the abundances of a number of elements derived from single lines are also in good agreement with the accepted values.

The iron abundance obtained here deserves closer examination. Photospheric iron abundances are often found to be much higher than the meteoric iron abundance. Other measurements find the photospheric abundance to be lower (close to the meteoric abundance).²² It is likely that a large part of the variation is due to different treatments of line broadening. The result obtained here is intermediate between the

²²See Blackwell, D.E., Lynas-Gray, A.E. and Smith, G. "On the Determination of the Solar Iron Abundance Using Fe I Lines" *Astronomy and Astrophysics* **296**, pg 217-232 (1995) and Holweger, H., Kock, M. and Bard, A. "On the Determination of the Solar Iron Abundance Using Fe I Lines - Comments on a Paper by Blackwell et al. and Presentation of New Results for Weak Lines" *Astronomy and Astrophysics* **296**, pg 233-240 (1995).

standard solar and meteoric abundances. The abundance obtained for iron through a non-plane-parallel analysis will be of interest in resolving this (see section 8.3.6).

As the abundance obtained from a particular line is strongly affected by the oscillator strength of the line, the errors in the abundances obtained could be reduced by using more accurate oscillator strengths. This would require either experimental measurement of oscillator strengths, or improvements in theoretical methods. The determination of oscillator strengths is discussed in Appendix A, and an experiment to measure oscillator strengths is described in Appendix B.

It is also possible, given accurate photospheric abundances, to determine oscillator strengths from these abundances. Such determinations can be useful as a check of the accuracy of theoretical or experimental values, or can be used directly when examining the spectra of other stars. Determinations of such “astrophysical” f -values can be readily found in the literature (a small number were determined in the course of this work), but they are of little use when attempting to determine solar abundances of elements.

